Polarity-tuned Gel Polymer Electrolyte Coating of High-voltage LiCoO$_2$ Cathode Materials

Jang-Hoon Park, Ju-Hyun Cho, Jong-Su Kim[†], Eun-Gi Shim[†], Yun-Sung Lee[††], and Sang-Young Lee*

Department of Chemical Engineering, College of Engineering, Kangwon National University, Chuncheon, Kangwondo 200-701, Korea
[†]*Techno Semichem, Yongin, Gyeonggi 446-599, Korea*
[††]*School of Applied Chemical Engineering, Chonnam National University, Gwangju 500-757, Korea*

Abstract : We demonstrate a new surface modification of high-voltage lithium cobalt oxide (LiCoO$_2$) cathode active materials for lithium-ion batteries. This approach is based on exploitation of a polarity-tuned gel polymer electrolyte (GPE) coating. Herein, two contrast polymers having different polarity are chosen: polyimide (PI) synthesized from thermally curing 4-component (pyromellitic dianhydride/biphenyl dianhydride/phenylenediamine/oxydianiline) polyamic acid (as a polar GPE) and ethylene-vinyl acetate copolymer (EVA) containing 12 wt% vinyl acetate repeating unit (as a less polar GPE). The strong affinity of polyamic acid for LiCoO$_2$ allows the resulting PI coating layer to present a highly-continuous surface film of nanometer thickness. On the other hand, the less polar EVA coating layer is poorly deposited onto the LiCoO$_2$, resulting in a locally agglomerated morphology with relatively high thickness. Based on the characterization of GPE coating layers, their structural difference on the electrochemical performance and thermal stability of high-voltage (herein, 4.4 V) LiCoO$_2$ is thoroughly investigated. In comparison to the EVA coating layer, the PI coating layer is effective in preventing the direct exposure of LiCoO$_2$ to liquid electrolyte, which thus plays a viable role in improving the high-voltage cell performance and mitigating the interfacial exothermic reaction between the charged LiCoO$_2$ and liquid electrolytes.

Keywords : Lithium-ion batteries, High-voltage lithium cobalt oxide, Polarity, Gel polymer electrolyte coating, Polyimide, Ethylene-vinyl acetate copolymer

1. Introduction

As applications of lithium-ion batteries are vigorously expanded into new fields such as smart mobile devices, (hybrid) electric vehicles, and energy storage systems, where high-energy density and high-power density are generally prerequisites, the development of new cathode active materials capable of providing large reversible capacity is strongly demanded.[1-6] Among various cathode active materials, lithium cobalt oxide (LiCoO$_2$) has been the most widely used material in commercial lithium-ion batteries, owing to its facile preparation and well-balanced electrochemical performance.

Meanwhile, as a promising attempt to increase the

capacity of LiCoO$_2$, charging LiCoO$_2$ above the conventional voltage of 4.2 V has been proposed.[7-11] However, increasing the charge cut-off voltage entails confronting formidable challenges related to deterioration of cycle performance and thermal stability. This is mainly due to the undesirable interfacial reaction between the charged (i.e., delithiated) LiCoO$_2$ and liquid electrolyte. As a potential approach to resolve this problem of high-voltage charged LiCoO$_2$, surface modification of LiCoO$_2$ with metal oxides such as Al$_2$O$_3$, ZrO$_2$, MgO, and ZnO has been extensively investigated.[12-15] Unfortunately, the metal oxides, which are often discontinuously deposited onto LiCoO$_2$, tend to act as an inert layer regarding ionic conduction and also require complex, cost-consuming coating processes.

In the present study, instead of sticking to the

*E-mail: syleek@kangwon.ac.kr

aforementioned metal oxide-based coatings, we demonstrate a new approach to surface modification of LiCoO$_2$ by exploiting a concept of polarity-tuned gel polymer electrolyte (GPE) coating. GPEs, which consist of polymer matrices and liquid electrolytes, have attracted considerable attention in lithium-ion batteries due to their excellent ionic transport and low rates of safety failure.[16-19] From the viewpoint of facilitating surface coverage onto LiCoO$_2$ and lithium ion transport of the coating layers, a GPE coating is expected to be a promising attempt, as it can easily provide a continuous, lithium-ion conducting coating layer, in comparison to the traditional metal oxide coatings.

Herein, as representative examples of GPE coating layers, two contrast polymers are respectively chosen on the basis of their polarity: polyimide (PI) and ethylene-vinyl acetate copolymer (EVA). The PI is introduced by thermally curing 4-component polyamic acid deposited onto LiCoO$_2$, wherein the polyamic acid is composed of (pyromellitic dianhydride (PMDA)/ biphenyl dianhydride (BPDA)/phenylenediamine (PDA)/ oxydianiline (ODA)). PI is extensively used in various applications such as membranes, fuel cells, displays, and microelectronics, owing to its excellent chemical/mechanical stability and film-forming properties.[20-24] Meanwhile, as another GPE coating layer, EVA containing 12 wt%

vinyl acetate repeating unit, which is known to be less polar than polyamic acid,[25] is employed. This difference in the polarity between the polyamic acid and EVA is expected to significantly affect their respective interfacial affinity for LiCoO$_2$, which thus may play a crucial role in determining the structure of the resulting GPE coating layers. In order to ensure a successful and unique functioning of the GPE coating layers, both the PI and EVA must fulfill a prerequisite condition that they are not soluble in N-methyl pyrrolidone (NMP), a common solvent used for cathode fabrication.

Characteristics of the GPE coating layers, focusing on their thin film structure and ionic transport, are elucidated as a function of polymer polarity difference. Based on this comprehensive understanding of GPE coating layers, their influence on the electrochemical performance (specifically, discharge capacity, C-rate capability, cyclability, and cell impedance) and thermal stability of high-voltage (herein, 4.4 V) charged LiCoO$_2$ is investigated.

2. Experimental Details

2.1. Preparation of GPE-coated LiCoO$_2$

The chemical structures of the 4-component (PMDA/ BPDA/PDA/ODA) polyamic acid and EVA are depicted in Fig. 1. As the first step in the fabrication of PI-coated
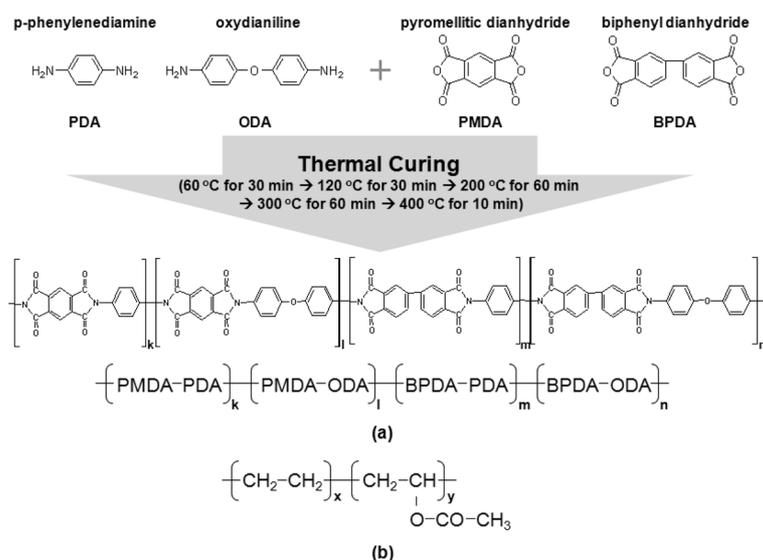

Fig. 1. Chemical structures of: (a) 4-component (pyromellitic dianhydride/biphenyl dianhydride/phenylenediamine/ oxydianiline) polyamic acid and resulting polyimide (PI); (b) ethylene-vinyl acetate copolymer (EVA) containing 12 wt% vinyl acetate repeating unit.

$LiCoO_2$, a polyamic acid solution was prepared using dimethylacetamide (DMAc) as a solvent under a nitrogen atmosphere. The polyamic acid concentration of the coating solution was 5 wt%. The molar ratio of diamines/dianhydrides in the solution was 1/1.01. The synthesis of polyamic acid has been described in greater detail in previous publications.[22,23] $LiCoO_2$ powders (average particle size = 10 um) were added to the polyamic acid coating solution, which was then stirred for 10 min and subsequently filtered. The filtered powders were dried at 30°C for 1 h and further vacuum-dried at 30°C for 4 h. In order to convert the polyamic acid into PI, the polyamic acid-coated $LiCoO_2$ powders were thermally cured via a stepwise imidization process (60°C for 30 min → 120°C for 30 min → 200°C for 60 min → 300°C for 60 min → 400°C for 10 min) under a nitrogen atmosphere.[24] Meanwhile, for the preparation of EVA-coated $LiCoO_2$, EVA (vinyl acetate = 12 wt%) was purchased from Aldrich and was dissolved in cyclohexane. The whole coating procedure, excluding the thermal imidization step, was identical to that of the aforementioned PI coating.

2.2. Characterization of GPE-coated LiCoO$_2$ and electrochemical performance of cells assembled with GPE-coated LiCoO$_2$

The surface morphology of the GPE-coated $LiCoO_2$ was examined using field emission scanning electron microscopy (FE-SEM, S-4300, Hitachi) and transmission electron microscopy (TEM, Tecnai G2 F30, FEI). For evaluation of the electrochemical performance of the GPE-coated $LiCoO_2$, $LiCoO_2$ cathodes were fabricated by coating a NMP-based slurry with a mixture of 95 wt% of $LiCoO_2$, 3 wt% of polyvinylidene fluoride (PVdF) binder, and 2 wt% of carbon black on an aluminum current collector. A unit cell (2032-type coin) was assembled by sandwiching a PE separator between a natural graphite anode and the GPE-coated $LiCoO_2$ cathode. The unit cell was then activated by being filled with a liquid electrolyte of 1 M $LiPF_6$ in ethylene carbonate (EC)/ethyl methyl carbonate (EMC) (= 1/2 v/v). The cell performance such as discharge capacity, C-rate capability, and cyclability was examined using battery test equipment (PNE Solution). The discharge current densities (i.e., discharge C-rates) were varied from 0.2 (= 0.59 mA cm^{-2}) to 2.0 C (= 5.87 mA cm^{-2}) at a constant charge current density of 0.2 C under a voltage range between 3.0 and 4.4 V. The cells were cycled at a constant charge/discharge current density of 0.5 C/0.5 C. The AC impedance of the 4.4 V-charged cells was measured using a VSP classic (Bio-Logic) over a frequency range of 10^{-2} to 10^6 Hz. The interfacial exothermic reaction between the charged $LiCoO_2$ cathode and liquid electrolyte was examined by differential scanning calorimetry (DSC, DuPont Q2000) measurements. The cells were charged to 4.4 V at a current density of 0.2 C and then disassembled in a dry room to remove the charged cathode. Approximately 10 mg of the cathode containing liquid electrolyte was hermetically sealed in a high-pressure DSC pan. The DSC measurements were performed in a temperature range from room temperature to 350°C at a heating rate of 10°C min^{-1} under a nitrogen atmosphere.

3. Results and Discussion

3.1. Structural characterization of GPE-coated LiCoO$_2$

The surface morphology of GPE-coated $LiCoO_2$ was characterized in Fig. 2. In comparison to the pristine $LiCoO_2$ (Fig. 2(a)), the PI coating layer is uniformly formed onto the $LiCoO_2$ surface and features a thin, highly-continuous morphology (Fig. 2(b)). On the other hand, the EVA coating layer is poorly deposited, resulting in a locally agglomerated structure with relatively high thickness (Fig. 2(c)). The polyamic acid is known to be more polar than the EVA,[25] which indicates that polyamic acid could be advantageous in delivering strong affinity for $LiCoO_2$. This benign compatibility of the polyamic acid toward $LiCoO_2$, in association with its outstanding film-forming capability,[20-23] may contribute to the realization of a highly-developed surface coverage of the PI coating layer onto the $LiCoO_2$ surface.[24]

This unusual PI coating layer was further characterized by conducting the TEM measurement. Fig. 2(d) shows that the $LiCoO_2$ is well covered by the PI coating layer with a thickness of approximately 10 nm, which demonstrates the evolution of the nanoarchitectured surface structure of the PI-coated $LiCoO_2$.

3.2. Electrochemical performance of cells assembled with GPE-coated LiCoO$_2$
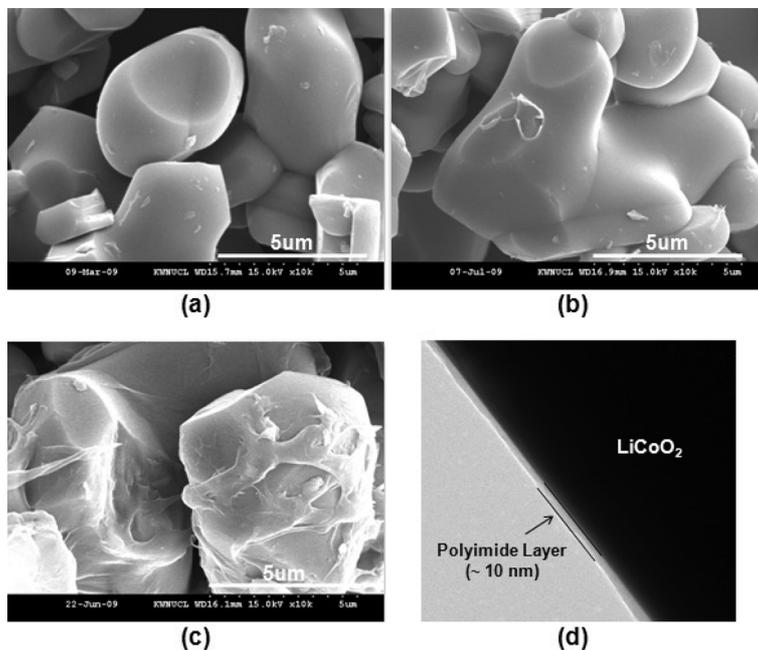
Fig. 3 depicts the effect of GPE coating layers on

Fig. 2. FE-SEM photographs of (a) pristine LiCoO₂; (b) PI-coated LiCoO₂; (c) EVA-coated LiCoO₂. (d) A TEM photograph of PI-coated LiCoO₂.
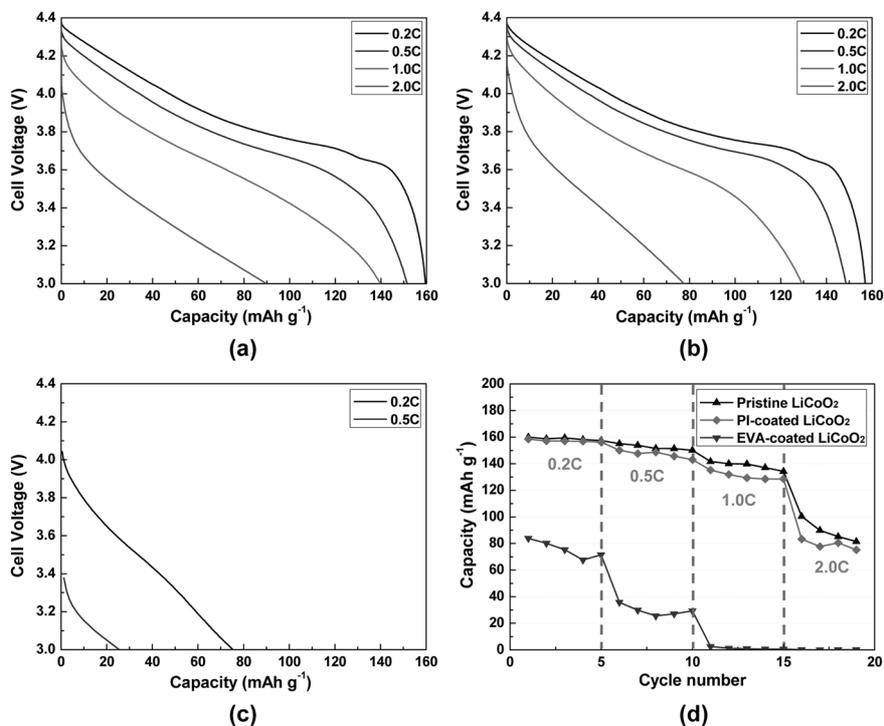

Fig. 3. Discharge profiles of cells charged to 4.4 V, where the discharge current densities are varied from 0.2 to 2.0 C at a constant charge current density of 0.2 C: (a) pristine LiCoO₂; (b) PI-coated LiCoO₂; (c) EVA-coated LiCoO₂. (d) Comparison of discharge capacities for various LiCoO₂ as a function of discharge current density.

the discharge profiles of cells charged to 4.4 V, wherein the discharge current densities were varied from 0.2 to 2.0 C at a constant charge current density of 0.2 C. The pristine $LiCoO_2$ shows a traditional voltage plateau and a discharge capacity of 160 mAh g^{-1} at a discharge current density of 0.2 C (Fig. 3(a)). Intriguingly, the discharge capacities of the PI-coated $LiCoO_2$ (Fig. 3(b)) are found to be comparable to those of the pristine $LiCoO_2$, although they are slightly lower at higher discharge current densities. On the other hand, a sharp voltage drop and very low discharge capacities are observed in the EVA-coated $LiCoO_2$ (Fig. 3(c)). This indicates that the EVA coating layer builds up a strong resistance to ionic conduction. Fig. 3(d) summarizes the discharge capacities of the pristine $LiCoO_2$ and GPE-coated $LiCoO_2$ as a function of discharge current density, i.e. discharge C-rate capability. It is of note that the difference in the discharge capacity between the PI- and the EVA-coated $LiCoO_2$ becomes larger at higher discharge current densities where the influence of ionic transport on the ohmic polarization (i.e., IR drop) is more pronounced.[26,27] The previous morphological characterization (Fig. 2) showed that the PI coating layer presents highly-continuous surface coverage of nanometer thickness (~10 nm), whereas the EVA coating layer is relatively thick and poorly deposited onto $LiCoO_2$. Meanwhile, a supplementary experiment for estimating the ionic conductivity of the GPE coating layers themselves (i.e., the liquid electrolyte (1 M $LiPF_6$ in EC/EMC = 1/2 v/v)-swelled PI (or EVA) film) was conducted. The PI-based GPE film (= 0.15 mS cm^{-1}) is observed to deliver higher ionic conductivity than the EVA-based GPE film (= 0.03 mS cm^{-1}). Hence, it is expected that this facile ion transport as well as the nanometer-thickness of the PI coating layer could contribute to superior discharge capacities and C-rate capability, as compared to the EVA coating layer. Schematic illustrations demonstrating the differences in the morphology and conceptual ion transport of the GPE coating layers are depicted in Fig. 5.

The effect of GPE-coated $LiCoO_2$ on the cycle performance, i.e. discharge capacity as a function of cycle number, of cells charged to 4.4 V was investigated. Fig. 4(a) shows that relative to the pristine $LiCoO_2$, the PI-coated $LiCoO_2$ provides significantly improved cycle performance. Up to the 40th cycle, there is little difference between the pristine $LiCoO_2$ and PI-coated $LiCoO_2$.

However, after the 40th cycle, whereas the discharge capacity of pristine $LiCoO_2$ continues to drop with an increase of cycle number, the capacity fading of the PI-coated $LiCoO_2$ is noticeably retarded. The capacity retentions after the 100th cycle are found to be 38% for the pristine $LiCoO_2$ and 76% for the PI-coated $LiCoO_2$, respectively. On the other hand, the discharge capacity of the EVA-coated $LiCoO_2$ sharply drops within only a few cycles, resulting in very poor cyclability.

In order to attain a better understanding of the influence of the GPE-coated $LiCoO_2$ on the cycle performance, the AC impedance spectra of 4.4 V-charged cells after the 1st, 50th, and 100th cycle were analyzed. It has been reported[7-10] that the semicircle of impedance spectra at the high frequency range can be ascribed to the resistance of the surface film on the electrode active materials and the semicircle observed at the medium-to-low frequency region can be attributed to the charge transfer resistance between the electrode active materials and liquid electrolyte. Fig. 4(b) shows that the cell impedance of the pristine $LiCoO_2$ significantly increases after the 100th cycle (Z_{Re}(100th cycle) − Z_{Re}(1st cycle) = $\Delta Z_{Re} > 1500$ ohm), wherein the inset depicts the variation of cell impedance at the relatively low impedance region. This indicates that the sharp capacity fading of the pristine $LiCoO_2$ could be related to an undesirable interfacial reaction between the charged $LiCoO_2$ and liquid electrolyte. Previous studies[7-15] reported that, predominantly due to liquid electrolyte decomposition at high voltages, a resistive layer could be formed onto the cathode active materials. The resistive layer may hinder ionic transport at the interface between the cathode active materials and liquid electrolyte, which thus would deteriorate the cycle performance of high-voltage charged cells.

Meanwhile, for the PI-coated $LiCoO_2$ (Fig. 4(c)), the increase of cell impedance is drastically suppressed (ΔZ_{Re} ~60 ohm). This demonstrates that the PI coating layer can effectively prevent the evolution of a resistive layer onto the 4.4 V-charged $LiCoO_2$ surface. This appears to be similar to the results obtained from traditional metal oxide coatings.[12-15] It has been reported that the improved cycle performance of metal oxide-coated $LiCoO_2$ is attributed to retardation of impedance growth between the $LiCoO_2$ and liquid electrolyte. In comparison, the EVA coating layer (Fig. 4(d)) presents a significantly large increase in the cell impedance after the 100th cycle ($\Delta Z_{Re} > 8000$ ohm), which is more severe compared to
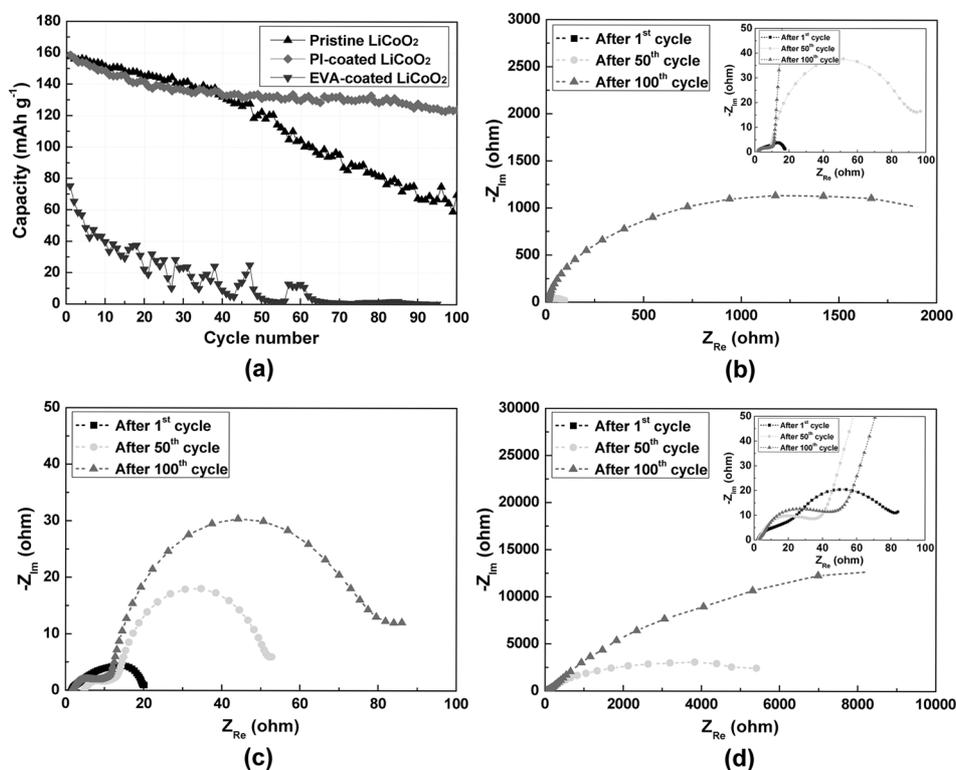
Fig. 4. (a) Discharge capacities as a function of cycle number for cells assembled with pristine $LiCoO_2$ or GPE-coated $LiCoO_2$, where cells are cycled at a constant charge/discharge current density (0.5 C/0.5 C) under a voltage range between 3.0 and 4.4 V. AC impedance spectra of 4.4 V-charged cells after the 1st, 50th, and 100th cycle: (b) pristine $LiCoO_2$; (c) PI-coated $LiCoO_2$; (d) EVA-coated $LiCoO_2$, wherein the insets depict the variation of cell impedance at the relatively low impedance region.

the impedance growth of pristine $LiCoO_2$. This indicates that the EVA coating layer, due to its poorly-developed morphology and sluggish ion transport, does not impede the rise of surface film resistance, but rather acts as a resistive layer to ionic conduction. As a consequence, the notorious deterioration in the discharge capacity, C-rate capability (Fig. 3), and cycle performance (Fig. 4) was encountered.

3.3. Analysis of interfacial exothermic reaction between GPE-coated $LiCoO_2$ and liquid electrolytes

Fig. 5 shows the DSC thermograms of the pristine $LiCoO_2$ and GPE-coated $LiCoO_2$ charged to 4.4 V. The pristine $LiCoO_2$ (Fig. 5(a)) delivers large exothermic heat ($\Delta H = 326$ J g^{-1}) and an exothermic peak temperature ($= 239°C$), which is attributed to the vigorous interfacial reaction of the charged $LiCoO_2$ with the liquid electrolyte.[7-11] In contrast, for the PI-coated $LiCoO_2$ (Fig. 5(b)), the exothermic heat is substantially reduced ($\Delta H =$
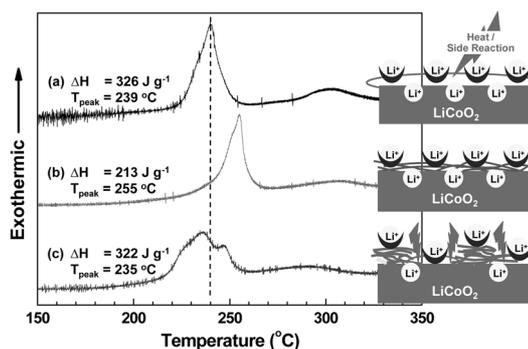

Fig. 5. DSC thermograms of interfacial exothermic reaction between 4.4 V-charged $LiCoO_2$ and liquid electrolyte: (a) pristine $LiCoO_2$; (b) PI-coated $LiCoO_2$; (c) EVA-coated $LiCoO_2$, wherein schematic illustrations demonstrating coating morphology, conceptual ion transport, and interfacial exothermic reaction of GPE-coated $LiCoO_2$ are inserted.

213 J g^{-1}) and the exothermic peak is also shifted to higher temperature ($= 255°C$). This indicates that the PI

coating layers effectively mitigate the surface exothermic reaction of the charged $LiCoO_2$ with the liquid electrolyte. On the other hand, the EVA-coated $LiCoO_2$ (Fig. 5(c)) fails to hinder the undesirable interfacial reaction, yielding large exothermic heat ($\Delta H = 322$ J g^{-1}) and relatively low peak temperature ($= 235°C$). This may be ascribed to the poor surface coverage of the EVA coating layer, implying that large surface area of $LiCoO_2$ is still exposed to the liquid electrolyte.

Schematic illustrations accounting for this intriguing thermal behavior of the pristine, PI-coated, and EVA-coated $LiCoO_2$ are also provided in Fig. 5. It is conceptually represented that the PI coating layer featuring the high surface coverage is effective in preventing $LiCoO_2$ from coming into direct contact with the violent liquid electrolyte, which leads to alleviating the interfacial exothermic reaction.

4. Conclusions

We investigated the effect of polarity-tuned gel polymer electrolyte coating on the cell performance and thermal stability of high-voltage (herein, 4.4 V) $LiCoO_2$. Owing to the strong affinity of polyamic acid for $LiCoO_2$, the resulting PI coating layer provided highly-continuous surface coverage of nanometer thickness ($\sim$10 nm). By contrast, the less polar EVA coating layer was poorly deposited onto the $LiCoO_2$ and thus showed locally agglomerated morphology with relatively high thickness. As a consequence, in comparison to the EVA coating layer, the nanostructured PI coating layer effectively prevented the direct exposure of $LiCoO_2$ to the liquid electrolyte, which contributed to suppressing the undesirable interfacial reaction. This unusual morphology of the PI coating layer, in association with its facile ionic transport, is advantageous in improving the high-voltage cell performance and mitigating the interfacial exothermic reaction of the 4.4 V-charged $LiCoO_2$ with the liquid electrolyte. The present study demonstrates that the structure of GPE coating layer, which is strongly affected by the polymer polarity, plays a crucial role in determining the electrochemical performance and thermal stability of high-voltage $LiCoO_2$.

Acknowledgment

References

1. J. Thomas, 'A spectacularly reactive cathode' *Nat. Mater.*, **2**, 705 (2003).
2. M. S. Whittingham, 'Lithium batteries and cathode materials' *Chem. Rev.*, **104**, 4271 (2004).
3. H. Li, Z. Wang, L. Chen, and X. Huang, 'Research on advanced materials for Li-ion batteries' *Adv. Mater.*, **21**, 4593 (2009).
4. M. R. Palacin, 'Recent advances in rechargeable battery materials: a chemist's perspective' *Chem. Soc. Rev.*, **38**, 2565 (2009).
5. B. L. Ellis, K. T. Lee, and L. F. Nazar, 'Positive electrode materials for Li-ion and Li-batteries' *Chem. Mater.*, **22**, 691 (2010).
6. J. B. Goodenough and Y. Kim, 'Challenges for rechargeable Li batteries' *Chem. Mater.*, **22**, 587 (2010).
7. K. S. Lee, Y. K. Sun, J. Noh, K. S. Song, and D. W. Kim, 'Improvement of high voltage cycling performance and thermal stability of lithium-ion cells by use of a thiophene additive' *Electrochem. Comm.*, **11**, 1900 (2009).
8. A. Abouimrane, I. Belharouak, and K. Amine, 'Sulfone-based electrolytes for high-voltage Li-ion batteries' *Electrochem. Comm.*, **11**, 1073 (2009).
9. Y. K. Sun, J. M. Han, S. T. Myung, S. W. Lee, and K. Amine, 'Significant improvement of high voltage cycling behavior AlF_3-coated $LiCoO_2$ cathode' *Electrochem. Comm.*, **8**, 821 (2006).
10. Y. K. Sun, S. W. Cho, S. T. Myung, K. Amine, and J. Prakash, 'Effect of AlF_3 coating amount on high voltage cycling performance of $LiCoO_2$' *Electrochim. Acta*, **53**, 1013 (2007).
11. D. Aurbach, B. Markovsky, A. Rodkin, E. Levi, Y. S. Cohen, H. J. Kim, and M. Schmidt, 'On the capacity fading of $LiCoO_2$ intercalation electrodes: the effect of cycling, storage, temperature, and surface film forming additives' *Electrochim. Acta*, **47**, 4291 (2002).
12. H. Miyashiro, A. Yamanka, M. Tabuchi, S. Seki, M. Nakayama, Y. Ohno, Y. Kobayashi, Y. Mita, A. Usami, and M. Wakihara, 'Improvement of degradation at elevated temperature and at high state-of-charge storage by ZrO_2 coating on $LiCoO_2$' *J. Electrochem. Soc.*, **153**, A348 (2006).
13. Z. Chen and J. R. Dahn, 'Methods to obtain excellent capacity retention in $LiCoO_2$ cycled to 4.5 V' *Electrochim. Acta*, **49**, 1079 (2004).
14. Z. Chen and J. R. Dahn, 'Effect of a ZrO_2 coating on the structure and electrochemistry of $LixCoO_2$ when cycled to 4.5 V' *Electrochem. Solid State Lett.*, **5**, A213 (2002).
15. W. Chang, J. W. Choi, J. C. Im, and J. K. Lee, 'Effects of ZnO coating on electrochemical performance and

thermal stability of LiCoO₂ as cathode material for lithium-ion batteries' *J. Power Sources*, **195**, 320 (2010).

16. J. Saunier, F. Alloin, J. Y. Sanchez, and G. Caillon, 'Thin and flexible lithium-ion batteries: investigation of polymer electrolytes' *J. Power Sources*, **119**, 454 (2003).

17. S. Y. Lee, W. H. Meyer, and G. Wegner, 'Phase behavior of gel-type polymer electrolytes and its influence on electrochemical properties' *ChemPhysChem*, **6**, 49 (2005).

18. A. M. Stephan, 'Review on gel polymer electrolytes for lithium batteries' *Eur. Polym. J.*, **42**, 21 (2006).

19. F. Ciuffa, F. Croce, A. Depifanio, S. Panero, and B. Scrosati, 'Lithium and proton conducting gel-type membranes' *J. Power Sources*, **127**, 53 (2004).

20. M. C. Choi, Y. K. Kim, and C. S. Ha, 'Polymers for flexible displays: From material selection to device applications' *Prog. Polym. Sci.*, **33**, 581 (2008).

21. L. Y. Jiang, Y. Wang, T. S. Chung, X. Y. Qiao, and J. Y. Lai, 'Polyimides membranes for pervaporation and biofuels separation' *Prog. Polym. Sci.*, **34**, 1135 (2009).

22. W. Essafi, G. Gebel, and R. Mercier, 'Sulfonated polyimide ionomers: a structural study' *Macromolecules*, **37**, 1431 (2004).

23. H. C. Liou, P. S. Ho, and R. Stierman, 'Thickness dependence of the anisotropy in thermal expansion of PMDA-ODA and BPDA-PDA thin films' *Thin Solid Films*, **339**, 68 (1999).

24. J. H. Park, J. S. Kim, E. G. Shim, Y. T. Hong, Y. S. Lee, and S. Y. Lee, 'Polyimide gel polymer electrolyte-nanoencapsulated LiCoO₂ cathode materials for high-voltage Li-ion batteries' *Electrochem. Comm.*, **12**, 1099 (2010).

25. J. Brandrup and E. H. Immergut, "*Polymer handbook 3rd edition*", Wiley, New York (1999).

26. H. S. Jeong, J. H. Kim, and S. Y. Lee, 'A novel poly (vinylidene fluoride-hexafluoropropylene)/poly(ethylene terephthalate) composite nonwoven separator with phase inversion-controlled microporous structure for a lithium-ion battery' *J. Mater. Chem.*, **20**, 9180 (2010).

27. J. H. Park, J. H. Cho, W. Park, D. Ryoo, S. J. Yoon, J. H. Kim, Y. U. Jeong, and S. Y. Lee, 'Close-packed SiO₂/poly (methyl methacrylate) binary nanoparticles-coated polyethylene separators for lithium-ion batteries' *J. Power Sources*, **195**, 8306 (2010).